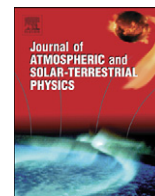




ELSEVIER

Contents lists available at SciVerse ScienceDirect

## Journal of Atmospheric and Solar-Terrestrial Physics

journal homepage: [www.elsevier.com/locate/jastp](http://www.elsevier.com/locate/jastp)

## Mesospheric intrusion and anomalous chemistry during and after a major stratospheric sudden warming

Ole-Kristian Kvissel<sup>a,\*</sup>, Yvan J. Orsolini<sup>b</sup>, Frode Stordal<sup>a</sup>, Varavut Limpasuvan<sup>c</sup>, Jadwiga Richter<sup>d</sup>, Dan R. Marsh<sup>d</sup>

<sup>a</sup> Department of Meteorology, University of Oslo, Oslo, Norway

<sup>b</sup> NILU - Norwegian Institute for Air Research, Kjeller, Norway

<sup>c</sup> Department of Chemistry and Applied Physics, Coastal Carolina University, Conway, South Carolina, USA

<sup>d</sup> National Center for Atmospheric Research (NCAR), Boulder, Colorado, USA

### ARTICLE INFO

#### Article history:

Received 1 November 2010

Received in revised form

29 August 2011

Accepted 30 August 2011

Available online 16 September 2011

#### Keywords:

Stratospheric sudden warming

Stratopause displacement

Whole Atmosphere Community Climate

Model

Ozone

### ABSTRACT

Several major stratospheric sudden warmings (SSWs) characterized by a rapid vertical displacement of the winter polar stratopause are simulated in the National Center for Atmospheric Research's Whole Atmosphere Community Climate Model. The stratopause descends into the mid-stratosphere at the onset of the SSW, and then abruptly reforms near 70 km. The SSWs are accompanied by a strong equatorward and downward residual circulation between 40 and 60 km. The descent occurs mainly through the core of the highly displaced vortex, and is accompanied by an intrusion of air rich in carbon monoxide (CO) from the mesosphere into the mid-stratosphere. Around the periods when the stratopause undergoes rapid vertical displacement, the simulation shows that the air of mesospheric origin is being cut off and remains distinct from surrounding stratospheric air masses for at least a month after SSW onset. Such mesospheric cut-off intrusion of CO-rich appears to be a defining signature of winters with major SSWs. Due to its strong temperature dependency, the secondary ozone maximum (between 90 and 110 km) abruptly decreases in amplitude at the time of the high-altitude stratopause reformation that influences the thermal structure at these altitudes. The vertical location of the tertiary ozone maximum (between 70 and 75 km) shows significant variations in response to the changing vertical motion during SSW.

© 2011 Elsevier Ltd. All rights reserved.

### 1. Introduction

A stratospheric sudden warming (SSW) is a dramatic middle atmosphere event that contributes significantly to the wintertime intra-seasonal variability (Andrews et al., 1987). According to WMO's definition, a major stratospheric sudden warming occurs when the zonal-mean zonal winds at 60°N and 10 hPa become easterly during winter. The event has traditionally been attributed to the enhancement of planetary wave disturbances and their interaction with the polar vortex (e.g. Matsuno, 1971). During such events, the polar stratosphere exhibits a warming of tens of degrees over a few days, and a weakening (i.e. minor SSW) or reversal (i.e. major SSW) of the winter polar westerlies. SSW events and their impacts on transport of minor constituents like carbon monoxide (CO), ozone (O<sub>3</sub>), nitrous oxide (N<sub>2</sub>O) and water vapor (H<sub>2</sub>O) have been readily observed by satellite instruments for several decades. For example, Manney et al. (2009b) describe a

recent SSW event in the winter 2008/09 and its impact on stratospheric transport. Polar mesospheric coolings have also been observed during SSWs, first by Labitzke (1972), and more recently by Thayer and Livingston (2008) using ground-based lidar observations at high latitudes, or by Siskind et al. (2005) using satellite observations by the Sounding of the Atmosphere using Broadband Emission Radiometry (SABER) instrument. Recent observations, both from the ground and from satellite, also reveal the existence of perturbed thermal and dynamical structures at yet higher altitudes in the upper mesosphere and lower thermosphere. During the strong 2009 SSW event, Funke et al. (2010) and Kurihara et al. (2010) noted an unusually warm layer at altitudes between 120 and 140 km, overlying the anomalously cool mesospheric layer. Disturbances in the ion temperature in the lower ionosphere have also been identified in mid-latitudes during the occurrence of a minor SSW event that occurred in 2008 (Goncharenko and Zhang, 2008). It is hence now clear that SSWs are dynamical disturbances affecting the entire middle and upper atmosphere, in addition to perturbing the tropospheric circulation (e.g. Baldwin and Dunkerton, 2001; Limpasuvan et al., 2004; Kolstad et al., 2010; Orsolini et al., 2011).

\* Corresponding author. Tel.: +47 22844071.

E-mail address: o.k.kvissel@geo.uio.no (O.-K. Kvissel).

Several recent studies using satellite observations reveal that some major SSWs are characterized by a sudden elevation of the polar stratopause. This extraordinary event is preceded by a prior descent of the polar stratopause and of the anomalous easterlies at the SSW onset. The descent of the polar stratopause during SSW onset has also been observed for several decades (Labitzke, 1972). For example, the stratopause descending by 30 km above Andøya (Northern Norway, 69°N) after an SSW in 1998 was reported by von Zahn et al. (1998). During such SSW events, a stratopause reforms at around 70 or 75 km, i.e. at standard mesospheric altitudes, and eventually descends to its climatological position (Siskind et al., 2007; Manney et al., 2008; 2009a,b; Smith et al., 2009; Orsolini et al., 2010). As the stratopause reforms at high altitudes, the upper stratosphere and lower mesosphere (USLM) are rapidly cooled by as much as 20 K, while the middle and upper mesosphere is warmed.

The onset of the SSW influences the downward transport of minor species in the winter vortex, which normally advects long-lived species with mesospheric abundances down to the lower stratosphere, e.g. Engel et al. (2006). The polar descent can become enhanced as the elevated stratopause returns to its climatological level during the recovery phase of the upper stratospheric polar vortex. For example, the enhanced descent of NO<sub>x</sub>, produced in the mesosphere and the thermosphere by energetic particle precipitation, following the recovery of the polar vortex after such major SSWs, has been clearly observed by satellites (Randall et al., 2006; Randall et al., 2009). After 2004 SSW observations revealed considerable O<sub>3</sub> depletion into the upper stratosphere linked to this NO<sub>x</sub> descent (Randall et al., 2005). The mesospheric descent also brings down air that is very dry and has high CO abundance into the polar stratosphere (Orsolini et al., 2010; Lee et al., 2011).

In addition, SABER satellite observations also show that, during such stratopause reformation events, the magnitude of the secondary ozone maximum (near 95 km) decreases, while the tertiary ozone maximum (near 70 km) intensifies and descends slightly (Smith et al., 2009).

In the recent years, three stratopause reformation events in 2004, 2006 and 2009 have been documented by satellite observations of the USLM thermal structure and composition (Manney et al., 2008; 2009a,b; Smith et al., 2009; Orsolini et al., 2010). However, there have been few studies of such events in global circulation models, e.g. Marsh (2011). Unraveling new chemical anomalies during such mesospheric descent events is potentially important to our understanding of O<sub>3</sub> variability and its role in climate change. To this end, this paper and the companion paper (Limpasuvan et al., in press) present the first detailed case study of a stratopause reformation event made with a comprehensive free-running chemistry–climate model.

In this study, we use a recent 50-year climate run of the National Center for Atmospheric Research (NCAR) Whole Atmosphere Community Climate Model (WACCM) to investigate in detail an SSW characterized by such a stratopause reformation. Previous WACCM simulations tended to generate an anomalously cold polar middle atmosphere, with an SSW frequency of occurrence smaller than observed. This new version with an improved parameterization of gravity waves and the inclusion of a turbulent mountain stress parameterization, is characterized by an SSW frequency of occurrence that matches closely the observed one, i.e. about 6 SSW per decade (Richter et al., 2010). Given a more realistic climatology of the middle atmosphere, the new WACCM runs serve as a useful tool to improve our understanding of an SSW.

We focus on a detailed dynamical and chemical study of an SSW event accompanied by a stratopause reformation, identified in this 50-year climate run. The model results during that

simulated event also provide insight on the dynamical forcing by gravity and planetary waves during the high-altitude stratopause reformation. This is the focus of the companion paper to the same Special Issue (Limpasuvan et al., in press).

## 2. Model and methodology

In this study, we focus on a major SSW identified in a 50-year long transient climate run, made with WACCM v3.5 for the chemistry–climate model validation exercise (CCMVal2) sponsored by the SPARC (Stratospheric Processes and their Role in Climate) program (SPARC CCMVal, 2010). The run covers the model years from 1955 to 2005, and is part of a four-member ensemble. The standard CCMVal2 runs output chemical species only every 10 days. Hence, a WACCM branch run was performed to cover a 6-month period around the chosen event, which occurred during the winter of model year 1979–80. Dynamical diagnostics and a suite of selected chemical species were archived every third hour throughout the simulated period.

WACCM covers the vertical region from the ground up to  $6.0 \times 10^{-6}$  hPa, i.e. to approximately 130 km geometric altitude, with 66 levels, and was run here at a horizontal resolution of  $1.9^\circ \times 2.5^\circ$  (latitude  $\times$  longitude). This transient run included solar forcing, i.e. auroral processes and solar proton events, and observed sea surface temperatures. Anthropogenic forcing is included in WACCM through tropospheric source species such as N<sub>2</sub>O, CH<sub>4</sub>, H<sub>2</sub>O, chlorofluorocarbons (CFCs) and other halogenated compounds. WACCM incorporates a detailed neutral chemistry for the middle atmosphere, that accounts for the evolution of 51 neutral species, including all the significant members of the O<sub>x</sub>, NO<sub>x</sub>, HO<sub>x</sub>, halogen chemical families and respective reservoir species (Kinnison et al., 2007). Heterogeneous processes on sulfate aerosols and polar stratospheric clouds are also included in the model. Further details can be found in Garcia et al. (2007), and references therein. Other model aspects covering ion chemistry, radiation and other processes relevant to aeronomy, are described in Marsh et al. (2007).

To understand the relative importance of various mechanisms that influence tracer transport, we examine the Transformed Eulerian Mean (TEM) circulation as described in Andrews et al. (1987). The TEM circulation has been post-processed from the 3-hourly model output fields. In several former studies the TEM circulation has been extensively used to describe wave-mean flow interaction, including episodes of SSWs such as Dunkerton et al. (1981) and Limpasuvan et al. (2004). It is the non-linear wave breaking and its associated wave vorticity fluxes that drive the TEM circulation. It represents an approximation of the wave forcing onto the zonal-mean flow. The role of forcing terms by resolved waves and by parameterized gravity waves and their effect on zonal-mean tendencies during the same event are examined in the companion paper (Limpasuvan et al., in press).

## 3. Stratopause reformation and intrusion of mesospheric air in the stratosphere

Fig. 1a,b shows the altitude–time cross-section of zonal-mean zonal wind ( $\bar{U}$ ) and the vertical component of the TEM circulation ( $\bar{w}^*$ ), respectively, from November model year 1979 to March model year 1980. Overlaid as black contours is the zonal-mean temperature. The fields have been averaged over the latitude band 63°–75°N, which straddles the latitude of the maximum zonal wind in early November, prior to the onset of the SSW. While pre-warming pulses occur in November and early December, the zonal-mean zonal wind reversal to easterlies occurs in

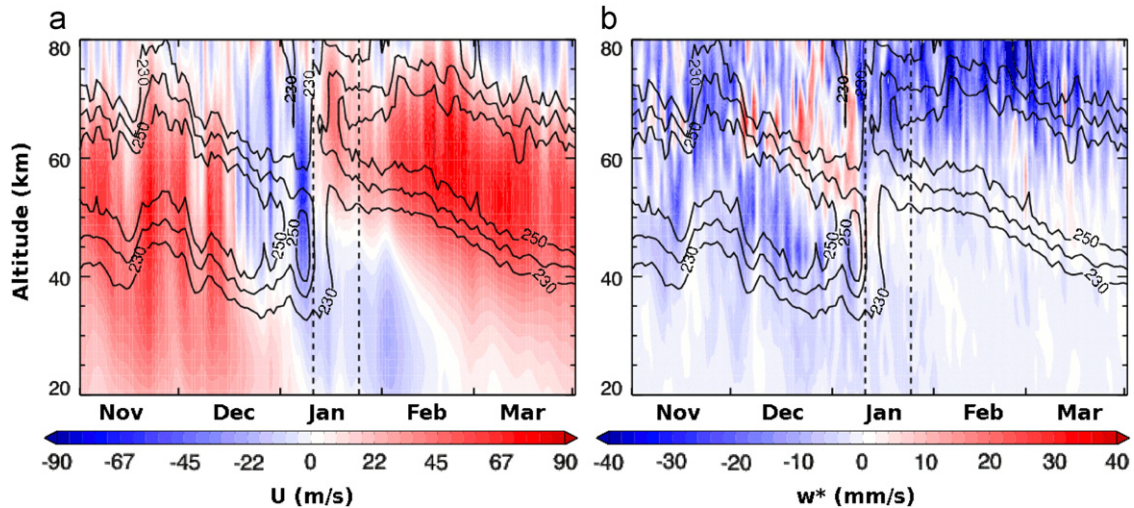


**Fig. 1.** Zonal-mean altitude–time cross-sections of  $\bar{U}$  (m/s) in (a),  $\bar{w}^*$  (mm/s) in (b) averaged over the latitude band ( $63^{\circ}$ – $75^{\circ}$ N), spanning from November 1 to the end of March.  $\bar{U}$  and  $\bar{w}^*$  are represented by colors (westerlies or upward: red; easterlies or downward: blue) and zonal-mean temperatures by black contour lines (every 10 K). The vertical dashed black lines correspond to January 11 and 25. In panel (a), the zero wind line corresponds to the transition between the light-blue and the white color shading. (For interpretation of the references to color in this figure legend, the reader is referred to the web version of this article.)

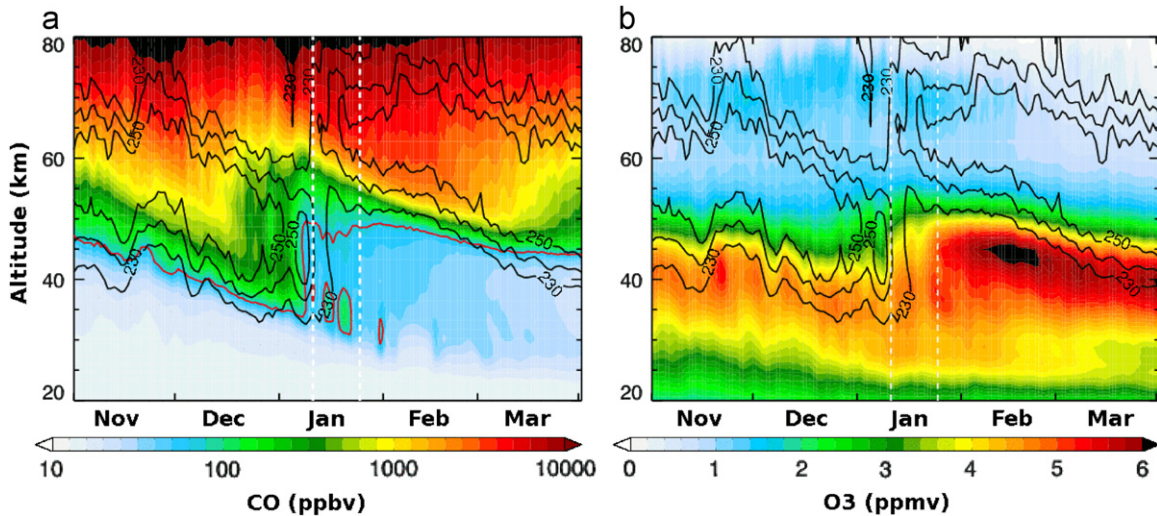


**Fig. 2.** Zonal-mean altitude–time cross-sections of CO (ppbv) in (a) and  $O_3$  (ppmv) in (b) averaged over the latitude band ( $63^{\circ}$ – $75^{\circ}$ N), spanning from November 1 to the end of March. Zonal-Mean temperatures are represented by black contour lines (every 10 K), while the vertical white dashed lines correspond to January 11 and 25. The red contour line in panel (a) corresponds to the 70 ppbv isopleth of CO. (For interpretation of the references to color in this figure legend, the reader is referred to the web version of this article.)

earnest by mid-December in the upper stratosphere and mesosphere. In early January, the easterly layer penetrates downward into the lower stratosphere.

In the period with easterly zonal-mean winds, a pattern of upward circulation emerges in the lower mesosphere, in the altitude range between  $\sim 45$  and 55 km, lasting until about January 11 and replacing the climatological downward circulation. The upward motion is associated with adiabatic cooling. In the upper stratosphere, on the contrary, downward motions prevail as seen in the descent of the easterly layer and of the polar stratopause. The date of January 11 indicates the time of the large and abrupt change in stratopause height. After the reformation of the stratopause at around 70 km, westerly zonal-mean winds and a downward TEM circulation are reestablished. A detailed examination of the dynamical forcing of the TEM circulation during and after the stratopause reformation is carried out in the companion paper (Limpasuvan et al., in press).

Next, we present in Fig. 2a,b altitude–time zonal-mean cross-sections of CO and  $O_3$  mixing ratios during the same period, also averaged over the latitude band  $63^{\circ}$ – $75^{\circ}$ N. The zonal-mean temperature is overlaid in black contours. Fig. 2a shows the gradual increase of CO in the middle and upper stratosphere early in the winter due to advection from the mesosphere. This enhanced downward tongue of CO is weakened from mid-December and interrupted around January 11, and the zonal-mean mixing ratios of CO in the middle and upper stratosphere decrease as the polar vortex breaks down and substantial meridional mixing advects CO-poor air poleward from mid-latitudes, resulting in a characteristic “hook-pattern” (Manney et al., 2009b). Throughout January, a series of CO maxima appear near 30–35 km in Fig. 2a near the tip of the descending CO tongue, and ultimately, a CO maximum becomes vertically cut off from it (as seen by the 70 ppbv CO isopleth contour). With the appearance of the elevated stratopause, a strong increase in polar

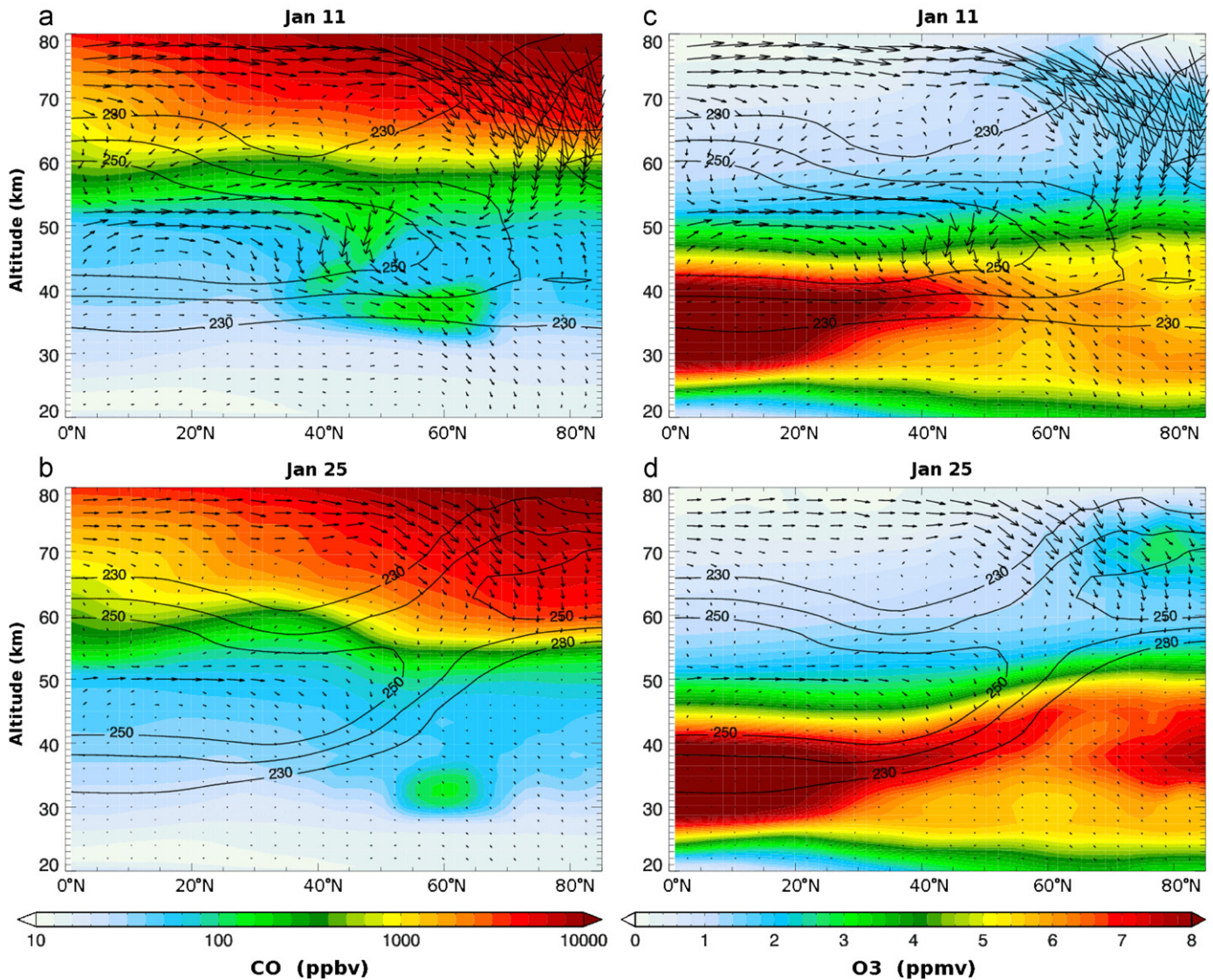


**Fig. 3.** Northern hemisphere zonal-mean meridional cross-sections of CO (ppbv) and O<sub>3</sub> (ppmv) on January 11 (a and c, respectively) and January 25 (b and d, respectively). Overlaid as black vectors is the TEM circulation, and as black contour lines is the zonal-mean temperature (every 10 K).

O<sub>3</sub> is evident between 40–50 km as shown in Fig. 2b. Further discussion about O<sub>3</sub> is made below.

Fig. 3a–d present zonal-mean meridional cross-sections of CO and O<sub>3</sub> on January 11 and 25. These dates correspond to the vertical, dash lines in Figs. 1 and 2. The horizontal and vertical components of the TEM circulation are overlaid as black vectors and the zonal-mean temperature as black contours. In Fig. 3a–b, the CO maximum is clearly seen as an intrusion collocated with strong residual descent between 30 and 50 km, and between 40°N and 60°N. The intrusion reflects the downward transport process in which the CO maximum is being cut off and isolated from the above reservoir. The correspondence between the diagnosed, post-processed TEM vectors and the CO behavior in the simulations demonstrates nicely the validity of the TEM approach. For example, the mid-latitude descending tongue of CO at 40–50 km in Fig. 4a coincides with strong downward residual velocities. By January 25, the CO-rich air originating from the mesosphere has been transported down with relatively little horizontal mixing, and is now fully surrounded by stratospheric air (Fig. 3b). The temperature contours in Fig. 3a,b shows that the polar stratopause, which is well separated from the mid-latitude stratopause

(Hitchman et al., 1989; Manney et al., 2009a; Orsolini et al., 2010), has reformed at an altitude of approximately 70 km and is beginning its descent. Note how, on January 11, the TEM circulation vectors indicate strong descent, at the onset of the stratopause reformation. The cut-off intrusion of CO-rich air is not an artifact of zonal averaging, as clearly seen in Figs. 4a–f and 5a–f, which depict synoptic maps of CO and O<sub>3</sub> mixing ratios for January 11 and 25, respectively, on three model levels corresponding approximately to 51, 40 and 30 km. The overlaid black contours represent geopotential height. In Fig. 4b, we see that the CO-rich air is contained in a vortex that is displaced toward mid-latitudes and is vertically coherent from 30 to 40 km. On January 11, the coma-shaped descent of high CO has not reached 30 km yet, as indicated by the fact that the CO abundance at this level does not reflect a mesospheric origin. By January 25 (Fig. 5c), the CO-rich intrusion is now clearly seen in the vortex remnant in mid-latitudes at 30 km, and is vertically cut off from the reservoir above. The vortex remnant with mesospheric CO abundance remains distinct from surrounding stratospheric air for at least one month after the SSW was initiated. The high CO mixing ratios eventually decrease due to mixing with surrounding air masses

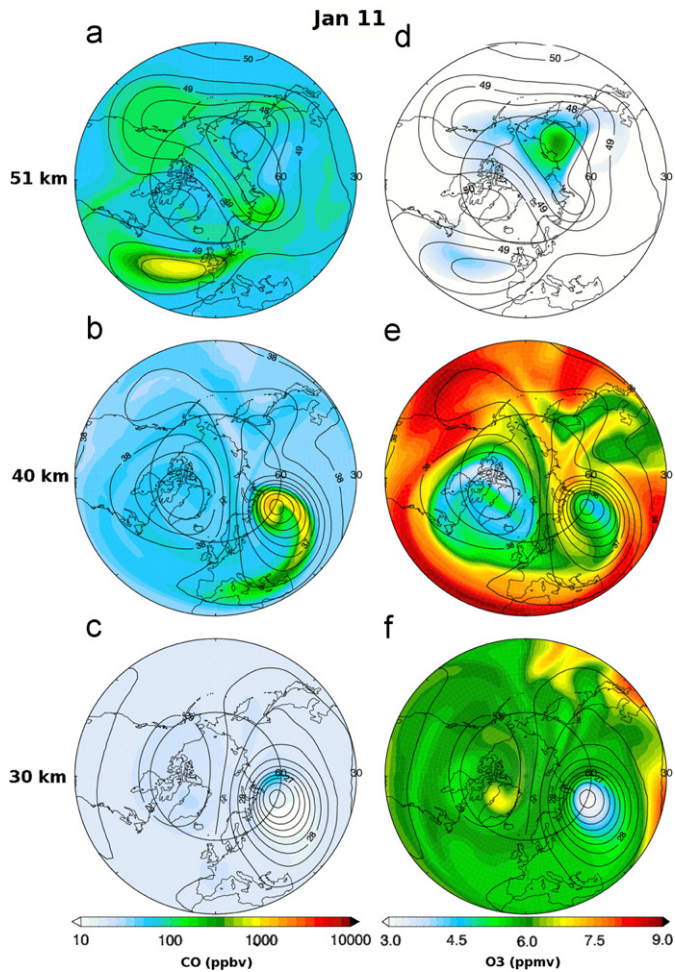


**Fig. 4.** Synoptic maps of CO (ppbv) and O<sub>3</sub> (ppmv) at 51 km (a and d, respectively), 40 km (b and e, respectively) and 30 km (c and f, respectively) on January 11. Overlaid as black contour lines is geopotential height. Contour intervals are 500 m in (a, d) and 250 m in (b, c, e, f). The black circle corresponds to 60°N.

(Fig. 2a), and possibly by chemical reaction with the hydroxyl radical (OH). At 51 km, the synoptic maps show clearly the vortex restrengthening by January 25 (Fig. 5a).

The cross-sections of O<sub>3</sub> in Figs. 2b and 3c,d nearly mirror those in CO, as O<sub>3</sub> has lower mixing ratios in the mesosphere than in the stratosphere. However, O<sub>3</sub> abundances are strongly influenced by the chemical reactions and by photolysis, and hence O<sub>3</sub> is not a dynamical tracer of mesospheric transport like CO. Hence, the O<sub>3</sub> signature in the vortex remnant in the process of being cut off is not as apparent as in CO (Fig. 3c,d). In Fig. 4e, at 40 km, there are two pools of low O<sub>3</sub>. The large pool in the western hemisphere arose from intruding air masses originating at low latitudes and mixed into the large anticyclone. Such low ozone pockets (LOP) in winter anticyclones have been previously discussed in the literature (Manney et al., 1995; Harvey et al., 2008). The LOP is characterized by low O<sub>3</sub> and low CO, as it originates at mid-stratospheric subtropical latitudes. The smaller low O<sub>3</sub> pool in the eastern hemisphere is confined to the vortex remnant displaced from the pole and carries the high-CO signature of mesospheric air. This pool of air has descended all the way from the mesosphere in about 10–20 days. It could only keep its mesospheric signature of O<sub>3</sub> because it has largely resided at high latitudes where O<sub>3</sub> has a long chemical lifetime during winter. In Fig. 5e, the enriched O<sub>3</sub> area during January 25 (dark red region) tends to reside over higher latitude band and is more localized near Europe than during January 11. This high-latitude O<sub>3</sub> enhancement is consistent

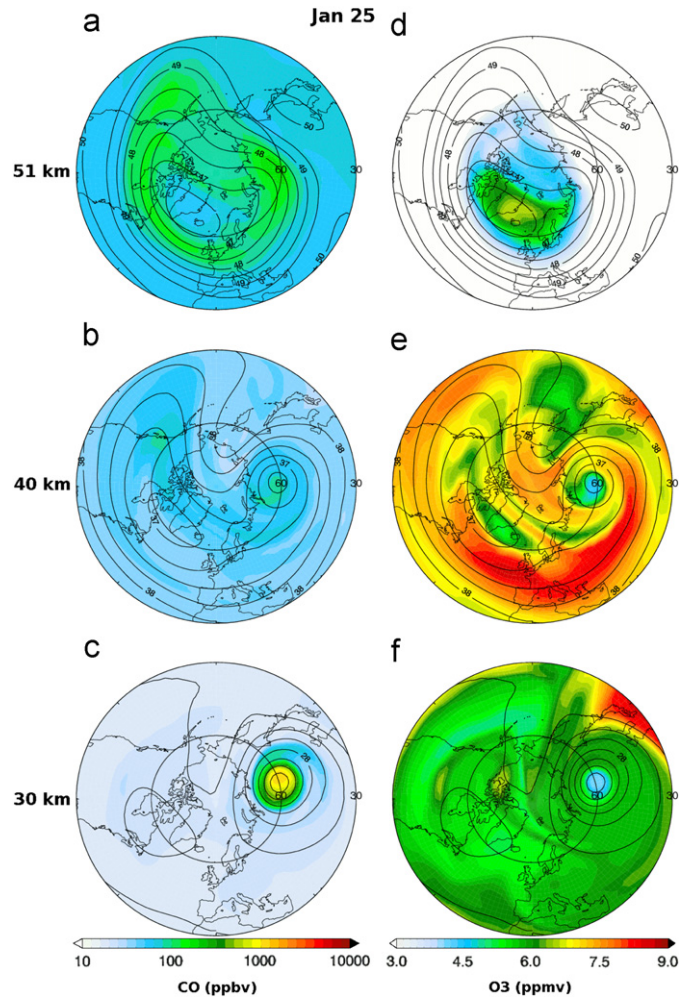


**Fig. 5.** Same as Fig. 4, except for January 25.

with the meridional structure between 35 and 45 km, as shown in Fig. 3d below the elevated stratopause.

#### 4. Mesospheric ozone maxima

The altitude–time evolution of zonal-mean O<sub>3</sub> and temperature are shown in Fig. 6a,b through the mesosphere–lower thermosphere, averaged over latitudes poleward of 70°N. As mesospheric O<sub>3</sub> has a strong diurnal cycle, only nighttime data is used, based on a threshold solar zenith angle of 95°. Overlaid as black contours is ( $\bar{w}^*$ ), averaged over the same latitudes. O<sub>3</sub> has a secondary maximum in the upper mesosphere, with production reactions involving combination of atomic oxygen and molecular oxygen, competing with loss reactions involving atomic oxygen and atomic hydrogen (Smith and Marsh, 2005). There is a negative correlation between O<sub>3</sub> and temperature at these altitudes due to temperature dependence of these reaction rates (e.g. Smith et al., 2009), as reflected in Fig. 6a,b. Comparing temperature with ( $\bar{w}^*$ ), it is clear that cold anomalies tend to coincide with ascent. The amplitude of the secondary ozone maximum around 95 km is remarkably reduced around January 11, when the stratopause elevation occurs. Polar-cap averaged O<sub>3</sub> decreases from mixing ratios as high as 6 ppmv prior to January 11 to values around 3 ppmv by the end of January. A similar reduction in percentage of the secondary ozone maximum was observed by Smith et al. (2009) in SABER data during the SSWs of

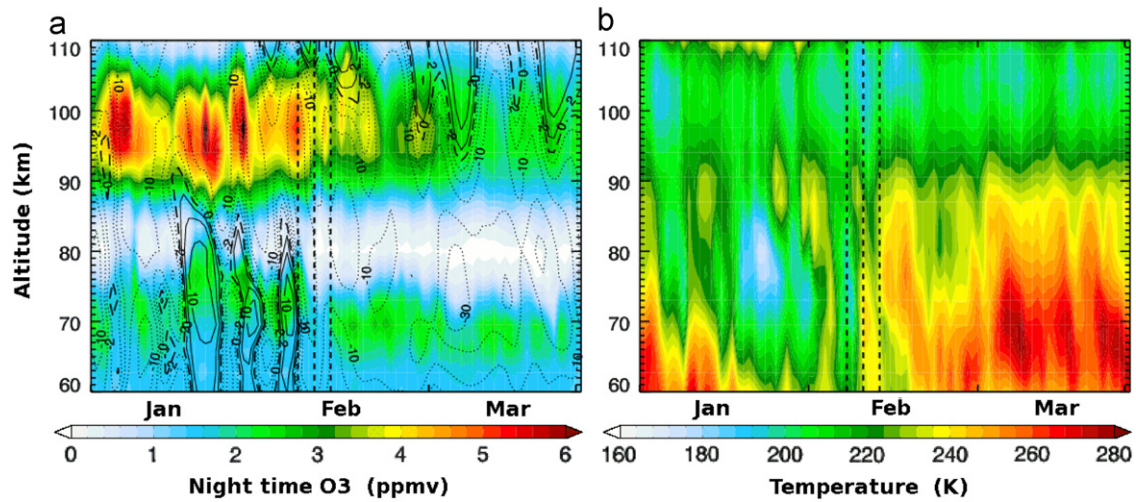


**Fig. 6.** Zonal-mean altitude–time cross-section of night-time  $O_3$  (ppmv) in (a) and temperature (K) in (b) averaged over latitudes poleward of  $70^\circ N$ , spanning from December 1 to the end of February.  $\bar{w}^*$  is represented by black contour lines in (a), dotted lines correspond to  $-2$ ,  $-5$ ,  $-10$ ,  $-20$ ,  $-30$  (mm/s), the dashed line is the zero line and the solid lines correspond to  $2$ ,  $5$ ,  $10$ ,  $20$ ,  $30$  (mm/s). The vertical black dashed lines correspond to January 8, 11 and 14.

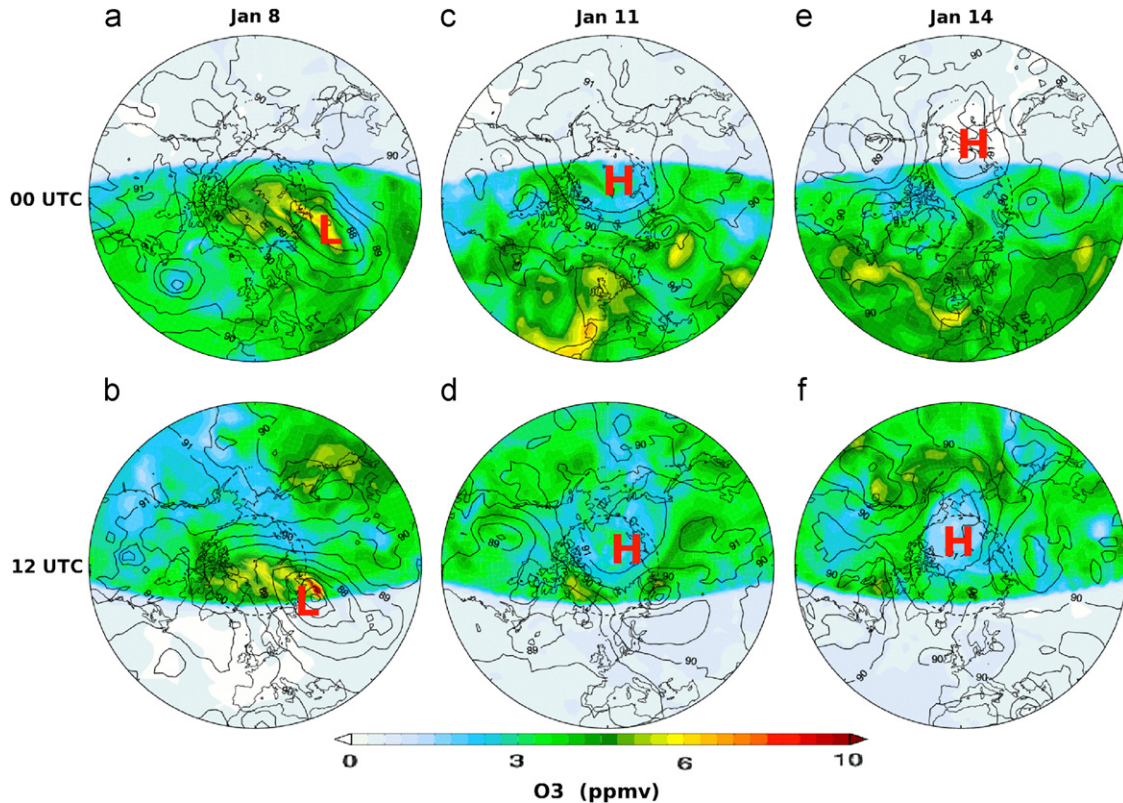


**Fig. 7.** Synoptic maps of  $O_3$  (ppmv) at 94 km on January 8 in (a, b), 11 in (c, d) and 14 in (e, f) at 00 UTC and 12 UTC, respectively. Overlaid as black contour lines is geopotential height with contour intervals of 500 m. The black dashed circle corresponds to  $70^\circ N$ . Low and high centers of geopotential height are marked with red capital letters.

2006 and 2009. Synoptic maps of  $O_3$  at 94 km are shown 12-hourly for January 8, 11 and 14 in Fig. 7a–f; the  $70^\circ N$  latitude circle, marking the southern boundary of the polar cap average in Fig. 6, is also shown. Nighttime values are much larger than daytime values. The decrease in the amplitude of the secondary maximum around January 11 (Fig. 6a) coincides with a low  $O_3$  pool straddling polar regions poleward of  $70^\circ N$  where an anticyclonic vortex (a geopotential height maximum) dominates (Fig. 7c–f). This period also marks the return of pre-warming easterlies at this

altitude and the occurrence of a high-latitude upper mesospheric planetary wave-1 (Limpasuvan et al., in press).

While periods of ascent in January above 100 km, and in February above 90 km are evident in Fig. 6a, the prevailing downward motion (negative  $\bar{w}^*$ ) persists on these three days around 94 km. Smith et al. (2009) explained that part of the  $O_3$  drop at these altitudes is attributable to the high mesospheric temperatures during this period. They also suggested that changes in the abundances of atomic oxygen and hydrogen are

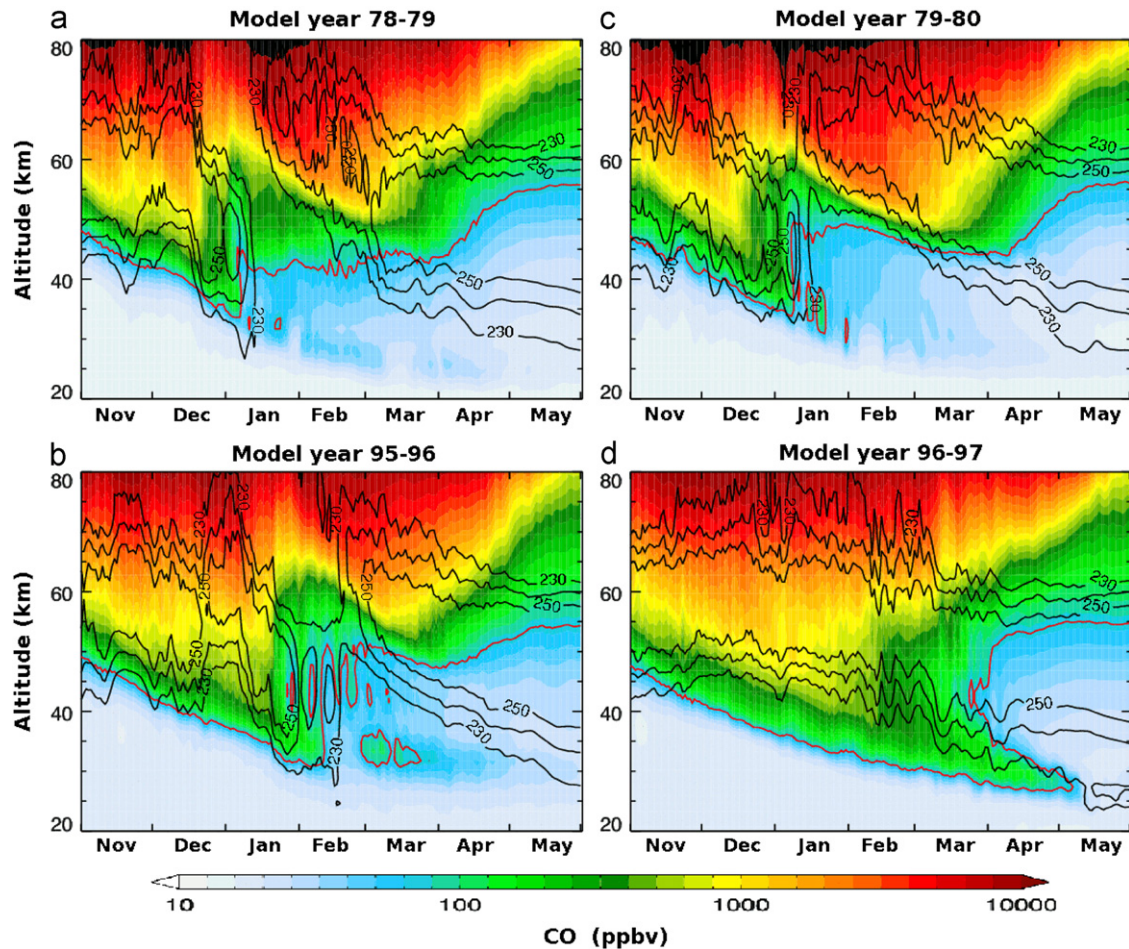


**Fig. 8.** Zonal-mean altitude–time cross-section of CO (ppbv) for four different cases: three NH winter seasons (model years 1978–79, 1995–96 and 1979–80) with SSWs in (a, b, c), and one (model year 1996–97) without SSW in (d). The red contour lines correspond to the 70 ppbv isopleth of CO.

needed to fully explain the lowered  $O_3$  amount. As shown in Fig. 6a, the weak polar-cap averaged descent around 94 km would not only warm the upper-mesosphere but also advect higher abundances of atomic oxygen and atomic hydrogen downwards. These combined influences can promote the  $O_3$  loss as suggested by Smith et al. (2009). Nevertheless, the chemistry of the secondary ozone maximum in our experiment needs further investigation, as the background  $O_3$  abundance in WACCM is lower than observed by SABER prior to the SSW.

Situated around 70 km, the tertiary ozone maximum is also affected by the stratopause reformation, as was also observed by SABER (Smith et al., 2009). Despite WACCM's low vertical resolution at these altitudes ( $\sim 3.5$  km), episodic upward shifts of the tertiary maximum location (by  $\sim 5$  km) occur prior to January 11 (Fig. 6a). These episodes coincide very well with the three ascent pulses and also with cooling, as also seen in Fig. 1 of Limpasuvan et al. (in press). With the return of downward motion after January 11, the tertiary ozone maximum then descends to its pre-warming altitude at about 70 km. The lowering (rising) of the tertiary maximum is consistent with the enhanced downward (upward) transport of  $O_3$ , which has a long photochemical lifetime at high latitudes during winter.

## 5. Year-to-year variability

Our study and the companion paper (Limpasuvan et al., in press) have focused on a high diagnostic frequency rerun and

analysis of the major SSW event in model year 1979–80, selected after the inspection of the 50-year WACCM CCMVal2 simulations. We have in fact examined a few additional events and, in this section, we present results from two additional winters with major SSWs (model year 1978–79 and model year 1995–96). We also contrast these events with one winter without SSW (model year 1996–97). For these four cases, Fig. 8 shows the altitude–time zonal-mean cross-sections of CO (color shading, and the 70 ppbv CO isopleth contour) and temperature (black contours), averaged over the latitude band  $63^\circ$ – $75^\circ$ N. During the three winters with major SSWs, we clearly see the abrupt mid-winter high-altitude reformation of the stratopause. In the three cases, the high-CO descent is interrupted, likely due to horizontal mixing with CO-poor air from lower latitudes during the SSW as shown in Fig. 5. A cut-off intrusion near the tip of the descending CO tongue is also apparent near 30 km, as was described in detail for the model year 1979–80 case. In model year 1996–97 winter (Fig. 8d), however, the stratopause is stable throughout the winter, and the mesospheric descent is continuous until around the period when the final warming occurs. In this non-SSW case, a corresponding high-CO cut-off intrusion is also suggested during the final warming.

## 6. Summary

In the foregoing sections, we have documented a major stratospheric warming event accompanied by the reformation of a

high-altitude polar stratopause, and the associated perturbations in the circulation and chemistry of the stratosphere and the mesosphere, as the stratopause slowly descends back to its climatologically level near 1 hPa. Along with our companion paper, these results represent the first detailed case study of such an event in a comprehensive free-running chemistry–climate model. During a high-altitude stratopause reformation, we have shown that a mesospheric intrusion, with high CO abundances, unfolds and get cut-off from above, becoming totally encapsulated by stratospheric air. The high CO anomaly persists for several weeks after the separation from the mesospheric air aloft and is further transported toward mid-latitudes before dissipating. While we have focused mainly on one event in model year 1979–80, we have shown occurrences of similar cut-off intrusions in several other simulated major SSWs.

The high-altitude stratopause reformation clearly impacts the secondary and tertiary ozone maxima, located at approximately 95 and 70 km, respectively. The secondary ozone maximum shows an abrupt decrease (of approximately 25%) at the time of the abrupt polar stratopause elevation, in agreement with the percentage reduction estimated by Smith et al. (2009) based on SABER observations. For the tertiary ozone maximum, the primary effect manifests in a change in altitude of the O<sub>3</sub> peak and is strongly correlated to  $\bar{w}^*$  (upward during the onset of the SSW and then downward thereafter). The companion paper, Limpasuvan et al. (in press), investigates the role of gravity and planetary waves during the same simulated model year 1979–80 SSW.

## Acknowledgments

OKK, YOR and FS were supported by the Norwegian Research Council NORKLIMA Program (Project Arctic\_Lis #178629). OKK had a three week stay at NCAR supported by The Norwegian Research School in Climate Dynamics (ResClim). VL is supported in part by the Large Scale Dynamics Program at the National Science Foundation (NSF) under Award number ATM-0646672 and the National Aeronautics and Space Administration (NASA) Contract NNX07AR25G. Part of this work was done while VL was on sabbatical leave at the National Center for Atmospheric Research (NCAR), with administrative support from Coastal Carolina University.

## References

- Andrews, D.G., Holton, J.R., Leovy, C.B., 1987. *Middle Atmosphere Dynamics*. Academic Press, 490 pp.
- Baldwin, M.P., Dunkerton, T.J., 2001. Stratospheric harbingers of anomalous weather regimes. *Science* 294, 581–584.
- Dunkerton, T.J., Hsu, C.-P.F., McIntyre, M.E., 1981. Some Eulerian and Lagrangian diagnostics for a model stratospheric warming. *Journal of Atmospheric Science* 38, 819–843.
- Engel, A., Möbius, T., Haase, H.-P., Bönisch, H., Wetter, T., Schmidt, U., Levin, I., Reddman, T., Oelhaf, H., Wetzel, G., Grunow, K., Huret, N., Pirre, M., 2006. Observation of mesospheric air inside the arctic stratospheric polar vortex in early 2003. *Atmospheric Chemistry and Physics* 6, 267–282.
- Funke, B., López-Puertas, M., Bermejo-Pantaleón, D., García-Comas, M., Stiller, G.P., von Clarmann, T., Kiefer, M., Linden, A., 2010. Evidence for dynamical coupling from the lower atmosphere to the thermosphere during a major stratospheric warming. *Geophysical Research Letters* 37, L13803. doi:10.1029/2010GL043619.
- Garcia, R.R., Marsh, D.R., Kinnison, D.E., Boville, B.A., Sassi, F., 2007. Simulation of secular trends in the middle atmosphere, 1950–2003. *Journal of Geophysical Research* 112, D09301. doi:10.1029/2006JD007485.
- Goncharenko, L., Zhang, S.-H., 2008. Ionospheric signatures of sudden stratospheric warming: Ion temperature at middle latitude. *Geophysical Research Letters* 35, L21103. doi:10.1029/2008GL035684.
- Harvey, V.L., Randall, C.E., Manney, G.L., Singleton, C.S., 2008. Low-ozone pockets observed by EOS-MLS. *Journal of Geophysical Research* 113, D17112. doi:10.1029/2007JD009181.
- Hitchman, M.H., Gille, J.C., Rodgers, C.D., Brasseur, G.P., 1989. The separated polar winter stratopause: a gravity wave driven climatological feature. *Journal of Atmospheric Science* 46, 4310–4422.
- Kinnison, D.E., Brasseur, G.P., Walters, S., Garcia, R.R., Marsh, D.R., Sassi, F., Harvey, V.L., Randall, C.E., Emmons, L., Lamarque, J.F., Hess, P., Orlando, J.J., Tie, X.X., Randel, W., Pan, L.L., Gettelman, A., Granier, C., Diehl, T., Niemeier, U., Simmons, A.J., 2007. Sensitivity of chemical tracers to meteorological parameters in the MOZART-3 chemical transport model. *J. Geophys. Res.* 112, D20302. doi:10.1029/2006JD007879.
- Kolstad, E.W., Breiteig, T., Scaife, A.A., 2010. The association between stratospheric weak polar vortex events and cold air outbreaks in the Northern Hemisphere. *Quarterly Journal of the Royal Meteorological Society* 136, 886–893. doi:10.1002/qj.620.
- Kurihara, J., Ogawa, Y., Oyama, S., Nozawa, S., Tsutsumi, M., Hall, C.M., Tomikawa, Y., Fujii, R., 2010. Links between a stratospheric sudden warming and thermal structures and dynamics in the high-latitude mesosphere, lower thermosphere, and ionosphere. *Geophysical Research Letters* 37, L13806. doi:10.1029/2010GL043643.
- Labitzke, K., 1972. Temperature changes in the mesosphere and stratosphere connected with circulation changes in winter. *Journal of Atmospheric Science* 29, 756–766.
- Lee, J.N., Wu, D.L., Manney, G.L., Schwartz, M.J., Lambert, A., Livesey, N.J., Minschwaner, K.R., Pumphrey, H.C., Read, W.G., 2011. Aura microwave limb sounder observations of the polar middle atmosphere: dynamics and transport of CO and H<sub>2</sub>O. *Journal of Geophysical Research* 116, D05110. doi:10.1029/2010JD014608.
- Limpasuvan, V., Thompson, D.W.J., Hartmann, D.L., 2004. The life cycle of Northern Hemisphere sudden stratospheric warmings. *Journal of Climate* 17, 2584–2596.
- Limpasuvan, V., Richter, J.H., Orsolini, Y.J., Stordal, F., Kvissel, O.-K. The roles of planetary and gravity waves during a major stratospheric sudden warming as characterized in WACCM. *Journal of Atmospheric and Solar-Terrestrial Physics*, 10.1016/j.jastp.2011.03.004. In press.
- Manney, G.L., Froidevaux, L., Waters, J.W., Zurex, R.W., Gille, J.C., Kurner, J.B., Mergenthaler, J.L., Roche, A.E., O'Neill, A., Swinbank, R., 1995. Formation of low-ozone pockets in the stratospheric anticyclone during winter. *Journal of Geophysical Research* 100 (D7), 13939–13950.
- Manney, G.L., Krüger, K., Pawson, S., Minschwaner, K., Schwartz, M.J., Daffer, W.H., Livesey, N.J., Mlynczak, M.G., Remsberg, E.E., Russel III, J.M., Waters, J.W., 2008. The evolution of the stratopause during the 2006 major warming: data and assimilated meteorological analyses. *Journal of Geophysical Research* 113, D11115. doi:10.1029/2007JD009097.
- Manney, G.L., Harwood, R.S., MacKenzie, I.A., Minschwaner, K., Allen, D.R., Santee, M.L., Walker, K.A., Hegglin, M.I., Lambert, A., Pumphrey, H.C., Bernath, P.F., Boone, C.D., Schwartz, M.J., Livesey, N.J., Daffer, W.H., Fuller, R.A., 2009a. Satellite Observations and Modelling of Transport in the Upper Troposphere through the Lower Mesosphere During the 2006 Major Stratospheric Sudden Warming. *Atmospheric Chemistry and Physics* 9, 4775–4795.
- Manney, G.L., Schwartz, M.J., Krueger, K., Santee, M.L., Pawson, S., Lee, J.N., Daffer, W.H., Fuller, R.A., Livesey, N.J., 2009b. Aura microwave limb sounder observations of dynamics and transport during the record-breaking 2009 arctic stratospheric major warming. *Geophysical Research Letters*, 36. doi:10.1029/2009GL038586.
- Marsh, D.R., Garcia, R.R., Kinnison, D.E., Boville, A., Sassi, F., Solomon, S.C., Matthes, K., 2007. Modeling the whole atmosphere response to solar cycle changes in and geomagnetic forcing. *Journal of Geophysical Research* 112, D23306. doi:10.1029/2006JD008306.
- Marsh, D.R., 2011. Chemical-dynamical coupling in the Mesosphere and Lower Thermosphere, in *Aeronomy of the Earth's Atmosphere and Ionosphere*, IAGA Special Sopron Book Ser., vol. 2, In: M. Abdu, D. Pancheva, A. Bhattacharyya, (Eds.), 1st ed., 370 pp., ISBN: 978-94-007-0325-4, Springer, Dordrecht, in press.
- Matsuno, T., 1971. A dynamical model of the stratospheric sudden warming. *Journal of Atmospheric Science* 28, 1479–1494.
- Orsolini, Y.J., Urban, J., Murtagh, D.P., Lossow, S., Limpasuvan, V., 2010. Descent from the polar mesosphere and anomalously high stratopause observed in 8 years of water vapor and temperature satellite observations by the odin sub-millimeter radiometer. *Journal of Geophysical Research* 115, D12305. doi:10.1029/2009JD013501.
- Orsolini, Y.J., Kindem, I.T., Kvamstø, N.G., 2011. On the potential impact of the stratosphere upon seasonal dynamical hindcasts of the North Atlantic oscillation: a pilot study. *Climate Dynamics*, 36. doi:10.1007/s00382-009-0705-6.
- Randall, C.E., Harvey, V.L., Manney, G.L., Orsolini, Y.J., Codrescu, M., Sioris, C., Brohede, S., Haley, C.S., Gordley, L.L., Zawodny, J.M., Russel III, J.M., 2005. Stratospheric effects of energetic particle precipitation in 2003–2004. *Geophysical Research Letters* 32, L05802. doi:10.1029/2004GL022003.
- Randall, C.E., Harvey, V.L., Singleton, C.S., Bernath, P.F., Boone, C.D., Kozyra, J.U., 2006. Enhanced NO<sub>x</sub> in 2006 linked to strong upper stratospheric Arctic vortex. *Geophysical Research Letters* 33, L18811. doi:10.1029/2006GL027160.
- Randall, C.E., Harvey, V.L., Siskind, D.E., France, J., Bernath, P.F., Boone, C.D., Walker, K.A., 2009. NO<sub>x</sub> descent in the Arctic middle atmosphere in early 2009. *Geophysical Research Letters*, L18811. doi:10.1029/2009GL039706.
- Richter, J.H., Sassi, F., Garcia, R.R., 2010. Towards a physically based gravity wave source parameterization. *Journal of Atmospheric Science*, 67. doi:10.1175/2009JAS3113.1.
- Siskind, D.E., Coy, L., Espy, P., 2005. Observations of stratospheric warmings and mesospheric coolings by the TIMED SABER instrument. *Geophysical Research Letters* 32, L09804. doi:10.1029/2005GL022399.

- Siskind, D.E., Eckermann, S.D., Coy, L., McCormack, J.P., Randall, C.E., 2007. On recent interannual variability of the Arctic winter mesosphere: implications for tracer descent. *Geophysical Research Letters* 34, L09806. doi:10.1029/2007GL029293.
- Smith, A.K., Marsh, D.R., 2005. Processes that account for the ozone maximum at the mesopause. *Journal of Geophysical Research* 110, D23305. doi:10.1029/2005JD006298.
- Smith, A.K., López-Puertas, M., García-Comas, M., Tukiainen, S., 2009. SABER observations of mesospheric ozone during NH late winter 2002–2009. *Geophysical Research Letters* 36, L23804. doi:10.1029/2009GL040942.
- S.P.A.R.C. CCMVal, 2010. SPARC Report on the Evaluation of Chemistry–Climate Models, In: V. Eyring, T.G. Shepherd, D.W. Waugh (Eds.), SPARC Report No. 5, WCRP-132, WMO/TD-No. 1526, <<http://www.atmos.physics.utoronto.ca/SPARC>>.
- Thayer, J.P., Livingston, J.M., 2008. Observations of wintertime arctic mesosphere cooling associated with stratosphere baroclinic zones. *Geophysical Research Letters* 35, L18803. doi:10.1029/2008GL034955.
- von Zahn, U., Fiedler, J., Naujokat, B., Langematz, U., Krüger, K., 1998. A note on recordhigh temperatures at the northern polar stratopause in winter 1997/98. *Geophysical Research Letters* 25 (22), 4169–4172. doi:10.1029/1998GL900091.